U. of Iowa 66-16

The Structure of the Solar Plasma Flow Generated by Solar Flares*

by

S.-I. Akasofu and S. Yoshida

Department of Physics and Astronomy
University of Iowa
Iowa City, Iowa

April 1966

*Research supported in part by grants from the National Aeronautics and Space Administration to the University of Alaska (NsG 201-62) and to the University of Iowa (NsG 233-62).

ABSTRACT

29739

Characteristics of geomagnetic storms caused by solar flares at different central meridian distances are statistically examined to obtain a two dimensional configuration of the solar plasma flow generated by solar flares.

It is shown that the front of the plasma flow is nearly semi-spherical, but its energy flux is greatly concentrated in a narrow cone from intense solar flares; therefore, the energy flux has a jet structure. It is shown that these results can be reasonably combined to give a consistent picture by assuming the generation of an interplanetary shock wave by the jet of the solar plasma ejected by a solar flare.

Author

1. Introduction

Let us suppose that a solar flare occurs at the point F indicated in Fig. 1. As seen from the earth, the position of the flare on the solar disk depends on the angle between the solar radii to F and to the earth. Let A be the position of the earth when the flare is seen on the central meridian. If the earth happens to be located at C, the flare is seen in the advancing (or commonly called the eastern hemisphere) and at B in the receding hemisphere (or the western hemisphere).

The purpose of this paper is to study statistically the two dimensional configurations of the solar plasma flow by examining characteristics of geomagnetic storms caused by solar flares in different sectors on the solar disk. A direct observation of this kind can be achieved by distributing space probes at different points on the earth's orbit, say the points B and C, together with the earth at A.

Such an attempt is by no means new; in fact, it has been well established that solar flares in the central meridian sector have the largest possibility of causing intense geomagnetic storms [cf. Obayashi and Hakura;[1] Bell;[2] Warwick and Haurwitz[3]].

However, most of the earlier studies used ΣK_p as an index of the intensity of geomagnetic storms. Unfortunately, the K_p index takes no account of the composition of the disturbance field (D), namely the compression field (DCF), the ring current field (DR), and the polar electrojet field (DP) and others, although the major contribution to large K_p indices is known to be due to the DP field. Recently, Yoshida and Akasofu[4] also examined this problem in the process of studying the absolute magnitude of solar flares.

In section 2 of this paper, we extend our earlier study to obtain accurately the magnitude of the storm sudden commencement (DCF) and of the main phase (DR) as a function of the central meridian distance of responsible solar flares. Our study is based on an extensive compilation [Yoshida[5]] of solar and geophysical events in which their causal relationship is confirmed by two independent studies [Warwick;[6,7] Obayashi[8]] and others.

In section 3 we obtain also the time elapsed between the onset time of solar flares and of resulting geomagnetic storms as a function of the central meridian distance of solar flares.

In section 4, all these results are combined to give a two dimensional configuration of an expanding solar plasma from the region of solar flares and support the view made by Gold[11] and recently Hirshberg[21] that a jet of the solar plasma ejected by a solar flare generates an interplanetary shock wave.

2. DCF and DR as a Function of the Central Meridian Distance

(a) DCF

Figure 2 shows the magnitude of storm sudden commencements and sudden impulses as a function of the central meridian distance. The quantity DCF is obtained by averaging the magnitude of storm sudden commencements (ssc) and sudden impulses (si) recorded at three stations widely separated in longitude: Honolulu (Hawii), San Juan (Puerto Rico), and Kakioka (Japan). The dot with circle indicates a ssc or si which is accompanied by the PCA and the dot not by the PCA; in general, solar flares which are associated with solar protons are more energetic than those without it.

The magnitude of DCF is expected to depend on many factors, such as the intensity of solar flares, conditions in interplanetary space. Further, the geocentric distance of the apex of the magnetospheric boundary just before the arrival of an enhanced flow of the solar plasma is also an important factor in determining the DCF magnitude.

In spite of this complexity, however, the envelope of the points shows a clear dependence of DCF on the central meridian

distance, which indicates that intense solar flares in the central meridian tend to cause a greater DCF than those in the other sectors.

Mead[9] has given the magnitude of the horizontal component δH of the magnetic field due to the compression of the earth's field;

$$\delta H = \frac{25000}{r_B^3} \quad (\gamma),$$

where r_B denotes the geocentric distance of the apex of the magnetospheric boundary. Let m, n, v be the mass, number density, and the velocity of the solar plasma, $p = 2\,mnv^2$ its pressure at the apex, B the intensity of interplanetary magnetic field and $p^* = p + B^2/8\pi$. By using the fact that at the apex the pressure p^* is balanced by the magnetic pressure $B_t^2/8\pi$ of the magnetosphere (where B_t is approximately twice as much as the earth's dipole field at $r = r_B$), the above equation may be rewritten as

$$\delta H \simeq 2\sqrt{p^*}\,.$$

Therefore, the pressure p^* is proportional to $(\delta H)^2$; note that p^* is expected to change by an order of magnitude. When this is taken into account, the dependence of the amount of the enhanced

pressure on the central meridian distance derived from Fig. 2 is quite remarkable. The ratio of the pressure at the point A to that at the point right angle to the line FA in Fig. 1 is as large as an order of magnitude.

(b) DR

Figure 3 shows the magnitude of the main phase decrease (DR) at the maximum epoch as a function of the central meridian distance. The quantity DR is obtained by using Sugiura's Dst (1963) values[10] for the IGY period, and for other periods by averaging the magnitude of the decrease at three stations, Honolulu, San Juan, and Kakioka.

A considerable scattering of the points is seen in the diagram. Nevertheless, the envelope shows again a remarkable dependence of the magnitude of the main phase decrease on the central meridian distance of solar flares.

(c) Magnetic Records

It is worthwhile to examine at this point records of actual geomagnetic storms caused by solar flares in different solar sectors. For this purpose, we have chosen first geomagnetic storms caused by solar flares whose importance was 3 or 3^+ and

which occurred at central meridian distances greater than 60° E or 60° W during the period 1956-1961. They are shown in the left column of Fig. 4 (Nos. 1 to 9); see also Table 1. In the middle and right columns, we show geomagnetic storms caused by flares whose importance was 3^-, 3, or 3^+ and which occurred at central meridian distances smaller than 15° E or 15° W during the same period.

Many of the geomagnetic storms caused by limb flares tend to have a small ssc and some a prolonged initial phase; the growth of the main phase is not always obvious. By contrast, central flares tend to cause a greater ssc and main phase decrease than limb flares. This becomes more obvious by noting the fact that some of the weaker storms (Nos. 11, 13, 19, 23, and 24) were caused by flares whose latitude was greater than 20°. This suggests that the magnitude of DCF and DR depends not only on the central meridian distance, but also on the latitude and that the scattering of the points in Figs. 2 and 3 is partly due to the latitude effect (although this point should be confirmed in the future after a more extensive compilation of the solar and geophysical events, taking into account the gradual equatorward shift of active regions

of the sun as the solar cycle progresses). Therefore, the energy for geomagnetic storms is confined in a narrow cone whose axis is the solar radial passing through flares, suggesting a jet-like structure of the plasma flow.

3. The Time Interval Elapsed Between the Onset Times of Solar Flares and Resulting Geomagnetic Storms

Figure 5 shows the time interval (t_s) elapsed between the onset times of a solar flare and of the resulting ssc. The solar disk is divided into six sectors, and the histogram of t_s is obtained for each sector.

It is clear that there is no definite relation between t_s and the central meridian distance of solar flares; in all sectors, ssc's occur in a wide range of t_s, but they are well confined between $20 < t_s < 70$ hours. Therefore, we are led to conclude that the front of the plasma flow causing ssc has a spherical front. This result is rather surprising since the results in section 2 suggest a jet-like structure of the solar plasma flow.

The accuracy of t_s for ssc must be of order a few minutes since both onset times are known with this accuracy. However, the onset time of DR is rather uncertain, particularly those caused by limb flares or high latitude flares. This can be easily recognized by examining some of the records in Fig. 4. By defining the onset time of the main phase to be the time

when the Dst value becomes less than the pre-storm level*, a tentative histogram is also constructed and is shown in Fig. 5. Again, the onset times are confined between 20 and 70 hours.

---

*Geomagnetic storms caused by western flares tend to develop the 'main phase' a few hours before the 'ssc', so that for those storms the onset time of DR is defined to be the time when the Dst values show the indication of the development of the decrease or when the activity of polar electrojet is enhanced.

4. Semi-Spherical Shock Wave Generated by a Jet of the Solar Plasma

(a) Figures 2, 3, and 5 indicate that the solar plasma flow generated from the region of solar flares can neither be a simple jet of the plasma nor a simple spherical (or spherically symmetric) wave.

(b) As Fig. 5 suggests, the front of the enhanced plasma flow is approximately semi-spherical. There are also some indication that solar flares which occur behind the limb of the sun can produce a definite sharp rise in the horizontal component of the geomagnetic field; for example, an intense solar flare, which occurred at (N28, W109), namely 19° behind the western limb at 2028 UT on November 20, 1960, produced a distinct sudden enhancement of the plasma pressure at 2147 UT on November 21 (see No. 8 in Fig. 4). Since the enhancement was not followed by any recognizable main phase (in agreement with Fig. 3), it has been classified as a sudden impulse (si), rather than a geomagnetic storm. Therefore, the sudden enhancement of the plasma pressure that causes a storm sudden commencement or a sudden impulse can occur even beyond a cone of solid angle π subtended at the location

of solar flares. This suggests that both ssc and si can be caused by an expanding wave, rather than by the actual solar gas ejected from the flare region.

(c) An important finding in the present work is that in spite of this spherical configuration, the pressure jump (causing ssc) across the front is large only in a limited part of the spherical surface, along the solar radius passing through a solar flare.

(d) Gold[11] was the first to suggest that ssc is caused by an interplanetary shock wave. Parker[12] examined the propagation of a spherically symmetric blast wave in a spherically symmetric medium. If the wave is generated by a sudden heating of the corona above the region of solar flares, the wave propagates in a nearly horizontally stratified medium whose density decreases rapidly radially upward from the photospheric surface, rather than in a spherically symmetric medium. The initial situation is more like a blast wave generated by a high altitude nuclear explosion; the wave front propagates first most rapidly radially upward [Colgate[13]]. The free expansion will, however, eventually occur after the wave propagates a certain distance from the sun, causing a roughly semi-spherically expanding wave beyond that

distance. Thus, at a distance of the earth's orbit, the blast wave will essentially be a semi-spherical wave, as Parker envisaged. From its nature, however, it is difficult to attribute the observed dependence of DCF on the central meridian distance to this type of simple spherical wave.

(e) A more likely situation would be the generation of a semi-spherical shock wave in the solar wind by a jet of the solar plasma ejected from the region of solar flares. The solar wind plasma will be most seriously compressed at the front of the advancing jet (causing the largest pressure jump and thus the largest ssc), but much less at the sides. The situation may be like a shock wave which is formed near the front of a blunt body moving supersonically. Figure 6 shows schematically the geometry of the shock wave generated in the quiet solar wind by the solar plasma ejected from the flare region [see Spreiter, Summer, and Aklsne[14]; their Fig. 18].

This gas dynamic consideration of the solar plasma flow is now justified by the fact that the observed geometry of the bow wave at the front of the magnetosphere agrees with the result of gas dynamic calculations by Spreiter and Jones.[15]

The geometry of the shock wave generated (in the quiet solar wind) by the solar plasma ejected at the time of a solar flare depends on various factors, such as the geometry of the solar plasma, its Mach number with respect to the quiet solar wind, the ratio of specific heat (γ), and the magnetic field ($\underline{B}$) [cf. Van Dyke,[16] Fuller,[17] Belotserkovskii and Chushkin[18]]. An application of this problem to interplanetary and magnetospheric problems has been discussed by Colburn and Sonett,[19] Spreiter, Summers, and Alksne,[14] and others.

The stand-off distance of the shock wave and the magnitude of the pressure jump across the wave depend also on the same parameters. For example, for a sphere of radius R and Mach number M, the stand-off distance Δ is of order 0.4 R, 0.25 R, and 0.18 R for M = 2, 3, and 4, respectively, for air ($\gamma = 7/5$). The pressure on the surface of the sphere varies rapidly as a function of θ which is the angle between the stagnation radius ($\theta = 0$) and an arbitrary radius. For the above values of M, the ratio of the pressure at $\theta = 45°$ to the stagnation pressure (at $\theta = 0°$) is of order 1/2. Thus, a serious compression of the interplanetary gas and a large pressure jump across the shock

wave occur only near the front of the advancing solar plasma. We conclude that the remarkable dependence of DCF on the central meridian distance is caused by this mechanism.

(f) The front of the advancing plasma can be described by either the contact discontinuity or the tangential discontinuity. The latter has been discussed by Dessler and Fejer,[20] Hirshberg,[22] and Colburn and Sonett[19] in connection with interactions between the M streams and the quiet solar wind.

When such discontinuities sweep across the magnetosphere, we would expect changes in the density ρ, speed v, or the magnetic field $\underline{B}$, and thus in their combined effect, namely changes in p* by a ground magnetometer. Some of the changes in $\underline{B}$ may be seen also in the Forbush decrease.

In order to examine this point, we have chosen geomagnetic storms with the main phase decrease of order 200 γ or more from selected storms in the Year Books (1935-1946, 1952-1955) from Kakioka Magnetic Observatory (Japan) and also from Catalogue of Disturbances (1956-1961) in Report on Ionosphere and Space Research in Japan; Fig. 7 and Table 2. This choice of the magnitude of 200 γ is made because they were likely to be caused by central flares (Fig. 3), and thus there is a great possibility of a direct

contact between the magnetosphere and the discontinuities (Fig. 6). It is quite obvious that many of the storms are far more complicated than what we expect from the concept of the average geomagnetic storm.

Some of them clearly have a double, triple, or multiple structure (namely, intense si activity) in the early phase of the storms; this feature was noticed by Newton and Milson.[23] Therefore, the discontinuity seems to have a complicated structure, rather than a simple one illustrated in Fig. 6. Such a fine structure seems to be a common feature for finite amplitude waves in a collisionless plasma [Morton[24]], although at present it is not possible to ignore the possibility of a multiple solar flare being the cause of such a complicated structure; note that many of the irregular features seen in the later phase of the storms are due to local ionospheric currents.

(g) Figure 8 shows the magnitude of the Forbush decrease as a function of the central meridian distance. One of the striking features is that the Forbush decrease of less than about 8% has a distribution of points similar to that shown in Figs. 2 and 3, while the points showing more than a 9% decrease are separated

from the above group. Further, nine cases out of 11 events were caused by eastern flares. This is not due to the lack of intense flares in the Western Hemisphere so that a large Forbush decrease (> 8%) has an east-west asymmetry [Sinno[25]].

In a simple situation, both the shock wave and the tangential discontinuity should be associated with the Forbush decrease since the tangential component (namely, the azimuthal component with respect to a solar radius) has a discontinuity there, and it is this discontinuity that affects the intensity of galactic cosmic rays behind it [cf. Parker[12]]. On the other hand, at a simple contact discontinuity, $\underline{B}$ should be continuous, so that we should not expect the Forbush decrease. However, the development of irregular features at the discontinuity could affect more seriously the cosmic ray intensity than a simple discontinuity [Haurwitz, Yoshida, and Akasofu[26]].

The symmetric part of the Forbush decrease in Fig. 8 is likely to be due to the shock wave in a way discussed by Parker,[12] by modifying his theory and taking into account the difference in the pressure jump at different points on the wave. The intense and asymmetric part may be explained in a way suggested by Haurwitz, Yoshida, and Akasofu;[26] it is due to a characteristic magnetic

field asymmetry that develops as a natural consequence of the interaction between the expanding solar plasma and the spiral type interplanetary magnetic field. It is thus not difficult to combine both features consistently in the structure of the plasma flow presented here. In Fig. 9, the distorted interplanetary magnetic fields are added to Fig. 6 to illustrate schematically the situation.

In fact, some of the intense Forbush decreases do not develop monotonically. For example, the geomagnetic storm of July 15, 1959, had a clear double structure in the Forbush decrease (Fig. 10). Yoshida and Akasofu[27] have shown recently that intense si activity during geomagnetic storms is more closely associated with the onset of intense Forbush decrease than a simple step-function type ssc. Such intense si activity may well be related to the discontinuities. Thus, a detailed comparison of both magnetic and cosmic ray records (such as Fig. 10) is quite important in understanding the structure of the plasma flow.

(h) The present study has not revealed any specific feature of the solar plasma flow as the cause of the main phase of geomagnetic storms. The main phase is characterized by the entry of the energy carried by the solar plasma flow into the magnetosphere, resulting

in the generation of the ring current deep in the trapping region and of a current system in the tail region and also of instabilities in the internal structure of the magnetosphere which are manifested by intermittent occurrence of the auroral and polar magnetic substorms.

It has already been shown, however, that an enhanced plasma pressure (or the kinetic energy flux) is not directly related in any obvious way to the growth of the main phase [Akasofu;[28] Dessler;[29] Akasofu and Chapman[30,31]]. The main phase can grow without a sudden enhancement of the plasma flow or even after a sudden decrease of it [Akasofu[32,33]]. Satellite observations show also that the time variations of the Kp indices are not related to the kinetic energy flux in any simple way [Wilcox and Ness[34]]. Therefore, it is too early to infer that the enhanced kinetic energy flux carried by the shock wave or by the discontinuity is directly responsible for the growth of the main phase.

It has also been clearly established that the growth of the main phase has no obvious relation to the Forbush decrease. Although they appear to grow together, a detailed examination of both magnetic and cosmic ray data shows that many storms with an intense main phase are not associated with the Forbush decrease and also that

many storms without any recognizable main phase are accompanied by a large Forbush decrease [Forbush;[35,36] Yoshida and Akasofu[27]]. Figure 11 shows such a contrasting pair of geomagnetic storms. In most cases, Forbush decreases last much longer than geomagnetic storms; for example, the Forbush decrease associated with the July 11, 1959, storm (Fig. 11) had continued until July 15 when a new Forbush decrease was superposed on it. Therefore, by observing the Forbush decrease and the main phase decrease, we see completely different aspects of the solar plasma flow. By observing the Forbush decrease, we see mainly distortions of interplanetary magnetic fields [cf. Parker;[12] Haurwitz, Yoshida, and Akasofu[26]]; by observing the main phase decrease, some unknown property of the plasma flow.

Further, as Fig. 5 shows, some of the western flares tend to cause the 'main phase' before the arrival of the shock wave (ssc). The onset of the 'main phase' can be seen as the onset of the activity of polar electrojet in polar magnetic records or as the onset of the decrease in the horizontal component of the earth's field. Fig. 12 shows an example in which a new activity of polar electrojets begins well before the onset of ssc seen in low latitudes.

It shows both College (representing a high latitude station) and Honolulu (representing a low latitude station) records on October 22/23 and 23/24, 1960. The ssc of October 24 storm was at 1452 UT (or 0452 College time and 0352 Honolulu time); it is marked by an arrow. The College record on October 23/24 shows that a new magnetic disturbance began at least four hours before the arrival of the shock wave, disrupting what had been a fairly calm period for at least 24 hours prior to the storm. Figure 13 shows a similar example. The ssc of the March 1, 1957, storm occurred at 1614 UT (or 0614 College time or 0514 Honolulu time); the College record on February 28/March 1 shows, however, that a new magnetic disturbance began at about 00 College time or a little earlier, at least six hours earlier than the ssc seen at Honolulu. An intense polar electrojet was observed between 0245 and 0430 College time, which caused a positive bay at Honolulu. This positive bay is due to the return current from the polar electrojet and is not due to an enhancement of the plasma pressure. This can be seen by examining magnetic records from stations widely distributed over the earth since positive bays appear only in a limited region of the earth, while ssc is seen over the entire earth. In these examples, the development of the 'main phase'

decrease is not clear, but there are a number of examples which show a simultaneous growth of both the electrojet and the 'main phase' decrease before the arrival of the shock wave. The most striking example is the storm of October 21/22, 1957; the shock wave arrived at about the maximum epoch of the 'main phase' decrease; an intense Forbush decrease then began.(37)

In spite of these complications, however, we believe that the remarkable dependence of the magnitude of DR on the central meridian distance is a new clue to explore the mechanism for the main phase of geomagnetic storms. In future papers, we plan to study the fine structure of the solar plasma flow along the line indicated in this paper, by using magnetic and cosmic-ray records taken simultaneously from a number of stations over the earth.

ACKNOWLEDGEMENTS

We would like to thank Dr. S. Chapman and Dr. J. A. Van Allen for their encouragement during the preparation of this paper. We are also indebted to Dr. John R. Spreiter and Mrs. Joan Hirshberg, Ames Research Center, NASA, for their helpful discussion. The work presented here was supported in part by grants from NASA to the University of Alaska (NsG 201-62) and to the University of Iowa (NsG 233-62).

REFERENCES

(1) Obayashi, T., and Y. Hakura, Propagation of solar cosmic rays through the interplanetary magnetic field, Rep. Ionosphere Space Res. Japan 14, 427-434 (1960).

(2) Bell, B., Major flares and geomagnetic activity, Smithsonian Contr. Astrophys. 5, 69-83 (1961).

(3) Warwick, C. S., and M. W. Haurwitz, A study of solar activity associated with polar cap absorption, J. Geophys. Res. 67, 1317-1332 (1962).

(4) Yoshida, S., and S.-I. Akasofu, A study of the propagation of solar particles in interplanetary space, Planet. Space Sci. 13, 435-448 (1965).

(5) Yoshida, S., A new classification of geomagnetic storms and their source flares, Scientific Rep. Geophysical Institute, Univ. of Alaska (August 1965).

(6) Warwick, C. S., National Bureau of Standards list of IGY flares with normalized values of importance and area, IGY Solar Activity Report Series No. 17 (1962).

(7) Warwick, C. S., Normalized solar flare data, July 1955 through June 1957, IGY Solar Activity Report Series No. 29 (1964).

(8) Obayashi, T., Table of solar geophysical events, July 1957--December 1960, Kyoto University, Kyoto, Japan (1962).

(9) Mead, G. D., Deformation of the geomagnetic field by the solar wind, J. Geophys. Res. 69, 1181-1195 (1964).

(10) Sugiura, M., Hourly values of equatorial Dst for the IGY, Goddard Space Flight Center Rept. (June 1963).

(11) Gold, T., Gas dynamics of cosmic clouds, I.A.U. Symposium Series, No. 2, North Holland Pub. Co., Amsterdam (1955).

(12) Parker, E. N., Sudden expansion of the corona following a large solar flare and the attendant magnetic field and cosmic-ray effects, Astrophys. J. 133, 1014-1033 (1961).

(13) Colgate, A., The phenomenology of the mass motion of a high altitude nuclear explosion, J. Geophys. Res. 70, 3161-3174 (1965).

(14) Spreiter, J. R., A. L. Summer, and A. Y. Alksne, Hydromagnetic flow around the magnetosphere, Planet. Space Sci. (1966).

(15) Spreiter, J. R., and W. P. Jones, On the effect of a weak interplanetary magnetic field on the interaction between the solar wind and the geomagnetic field, J. Geophys. Res. 68, 3555-3565 (1963).

(16) Van Dyke, M. D., The supersonic blunt-body problem--review and extension, J. Aeron. Sci. 25, 485-496 (1958).

(17) Fuller, F. B., Numerical solutions for supersonic flow of an ideal gas around blunt two-dimensional bodies, NASA Technical Note D-791 (1961).

(18) Belosterkorskii, O. M., and P. I. Chushkin, The numerical solution of problems in gas dynamics, Basic Developments in Fluid Dynamics, Vol. I, ed. by M. Holt, Academic Press (1965).

(19) Colburn, D. S., and C. P. Sonett, Discontinuities in the solar wind, Space Sci. Rev. (1966).

(20) Dessler, A. J., and J. A. Fejer, Interpretation of K index and M-region geomagnetic storms, Planet. Space Sci. 11, 505-512 (1963).

(21) Hirshberg, J., The relationship between solar wind velocities and surface magnetic disturbances during sudden commencement storms, J. Geophys. Res. 70, 4159-4163 (1965).

(22) Hirshberg, J., Recurrent geomagnetic storms and the solar wind, J. Geophys. Res. 70, 5353-5359 (1965).

(23) Newton, H. W., and A. S. Milson, J. Geophys. Res. 59 203 (1953).

(24) Morton, K. W., Finite amplitude compression waves in a collision-free plasma, Phys. Fluids 1, 1800-1815 (1964).

(25) Sinno, K., Mechanism of cosmic ray storms inferred from some statistical results, J. Phys. Soc. Japan 17, Suppl. A-II, 395-399 (1962).

(26) Haurwitz, M. W., S. Yoshida, and S.-I. Akasofu, Interplanetary magnetic field asymmetries and their effects on polar cap absorption events and Forbush decreases, J. Geophys. Res. 70, 2977-2988 (1965).

(27) Yoshida, S., and S.-I. Akasofu, The development of the Forbush decrease and the geomagnetic storm fields, Planet. Space Sci. (in press).

(28) Akasofu, S.-I., J. Geophys. Res. 65, 535-543 (1960).

(29) Dessler, A. J., J. Geophys. Res. 67, 4892-4894 (1962).

(30) Akasofu, S.-I., and S. Chapman, The development of the main phase of magnetic storms, J. Geophys. Res. 68, 125-129 (1963).

(31) Akasofu, S.-I., and S. Chapman, Magnetic storms: The simultaneous development of the main phase (DR) and of polar magnetic substorms (DP), J. Geophys. Res. 68, 3155-3158 (1963).

(32) Akasofu, S.-I., The development of geomagnetic storms after a negative sudden impulse, Planet. Space Sci. 12, 573-578 (1964).

(33) Akasofu, S.-I., The development of geomagnetic storms without a preceding enhancement of the solar plasma pressure, Planet. Space Sci. 13, 297-301 (1965).

(34) Wilcox, J. M., and N. F. Ness, Quasi-stationary corotating structure in interplanetary medium, J. Geophys. Res. 70, 5793-5803 (1965).

(35) Forbush, S. E., Terr. Mag. 43, 203-218 (1938).

(36) Forbush, S. E., World-wide cosmic-ray variations, 1937-1952, J. Geophys. Res. 59, 525-542 (1954).

(37) Ondoh, T., Ann. de Geophys. 18, 45-61, 1962.

TABLE 1

	Geomagnetic Storm Onset Time (ssc)	UT	Source Flare	UT		
1.	Mar. 25, 1958	1540	Mar. 23, 1958	0955	(S14 E78)	3^+
2.	July 11, 1959	1625	July 10, 1959	0206	(N22 E70)	3^+
3.	Dec. 7, 1960	1804	Dec. 5, 1960	1825	(N27 E68)	3^+
4.	July 20, 1961	0248	July 18, 1961	0920	(S08 W60)	3^+
5.	Apr. 9, 1959	1828	Apr. 8, 1959	0903	(N27 E85)	3
6.	Apr. 6, 1960	1628	Apr. 5, 1960	0215	(N12 W62)	3
7.	Sept. 4, 1960	1145	Sept. 3, 1960	0037	(N19 E89)	3
8.	Nov. 21, 1960	2147	Nov. 20, 1960	2028	(N28 W109)	3
9.	Mar. 27, 1961	1503	Mar. 26, 1961	1009	(S16 E75)	3

11.	Jan. 21, 1957	1950	Jan. 20, 1957	1850	(N14 E14)	3^-
12.	Sept.13, 1957	0046	Sept.11, 1957	0239	(N13 W04)	3^-
13.	Sept.21, 1957	1005	Sept.18, 1957	1818	(N20 E03)	3^+
14.	July 8, 1959	0748	July 7, 1958	0023	(N26 W05)	3
15.	Aug. 24, 1958	0140	Aug. 22, 1958	1422	(N18 W10)	3^-
16.	Mar. 26, 1959	0842	Mar. 24, 1959	0700	(N19 W04)	3
17.	Sept. 2, 1959	2159	Sept. 2, 1959	0720	(N13 W13)	3
18.	July 15, 1959	0803	July 14, 1959	0325	(N16 E07)	3^+
19.	Jan. 13, 1960	1859	Jan. 11, 1960	2040	(N23 E05)	3
20.	Apr. 1, 1960	0307	Mar. 30, 1960	1455	(N12 E13)	3^+
21.	Apr. 2, 1960	2313	Apr. 1, 1960	0843	(N15 W09)	3
22.	May 8, 1960	0421	May 6, 1960	1404	(S10 E08)	3^+
23	June 27, 1960	0145	June 25, 1960	1131	(N20 E07)	3
	June 27, 1960	1630	June 28, 1960	2039	(N19 W03)	3
24	Aug. 16, 1960	1409	Aug. 14, 1960	0511	(N24 W03)	3
25	Nov. 13, 1960	1200	Nov. 12, 1960	1315	(N26 W04)	3^+

TABLE 2

		UT
1.	Aug. 22, 1937,	02
2.	Apr. 16, 1938,	05
3.	Mar. 24, 1940,	13
4.	Mar. 1, 1941,	03
5.	July 5, 1941,	04
6.	Sept.18, 1941,	04
7.	Apr. 2, 1944,	04
8.	Mar. 28, 1946,	06
9.	July 26, 1946,	18
10.	Sept. 2, 1947,	23
11.	July 29, 1952,	19
12.	Jan. 5, 1953,	05
13.	Feb. 25, 1956,	02
14.	Jan. 21, 1957,	12
15.	Sept.13, 1957,	00
16.	Sept.29, 1957,	07
17.	Feb. 11, 1958,	01
18.	July 8, 1958,	07
19.	Sept. 4, 1958,	13
20.	July 15, 1959,	07
21.	Nov. 27, 1959,	23
22.	Mar. 31, 1960,	09
23.	Apr. 1, 1960,	08
24.	Apr. 30, 1960,	12
25.	Nov. 12, 1960,	13
26.	July 13, 1961,	10
27.	July 26, 1961,	19
28.	Sept.30, 1961,	18

FIGURE CAPTIONS

Figure 1. Relative location between the solar flare (F) and the earth.

Figure 2. Magnitude of storm sudden commencements and sudden impulses as a function of the central meridian distance of their responsible flares.

Figure 3. Magnitude of the main phase decreases as a function of the central meridian distance of their responsible flares.

Figure 4. (a) Left column: Geomagnetic storms caused by limb flares (central meridian distance > E 60° or W 60°) of importance 3 or 3^+.

(b) Central and Right columns: Geomagnetic storms caused by central flares (central meridian distance < E 15° or W 15°) or importance 3^-, 3, or 3^+. The records are the horizontal component traces from Honolulu observatory (1957, 1958, 1959, 1961) and from San Juan observatory (1960).

Figure 5. Time interval (t_s) elapsed between the onset times of a solar flare and of the resulting ssc (DCF). The solar disk is divided into six sectors, and the histogram of t_s is shown for each sector. The time interval for the onset of the main phase decrease (DR) is also shown in the same way; for the definition of the DR onset, see the text.

Figure 6. Proposed structure of the solar plasma flow generated by solar flares (schematic).

Figure 7. Intense geomagnetic storms with the main phase decrease of order 200 γ or more. The records are the horizontal component traces from Kakioka observatory.

Figure 8. Magnitude of Forbush decreases as a function of the central meridian distance of their responsible flares.

Figure 9. Distortion of interplanetary magnetic field (schematic) caused by the solar plasma flow illustrated in Fig. 6. A tangential discontinuity is assumed at the surface of the solar plasma.

Figure 10. Forbush decrease associated with the geomagnetic storm of July 15, 1959.

Figure 11. Contrasting pair of geomagnetic storms, together with the simultaneous cosmic-ray intensity. The upper storm was associated with an intense compression of the magnetosphere (but no definite main phase) and the Forbush decrease. The lower storm was associated with an intense main phase (but no ssc) and no recognizable Forbush decrease.

Figure 12. Onset of a new activity of polar electrojets before the storm sudden commencement of the October 24, 1960 storm. Both College (high latitude) and Honolulu (low latitude) magnetic records are shown.

Figure 13. Onset of a new activity of polar electrojets before the sudden commencement of the March 1, 1957 storm. Both College (high latitude) and Honolulu (low latitude) magnetic records are shown.

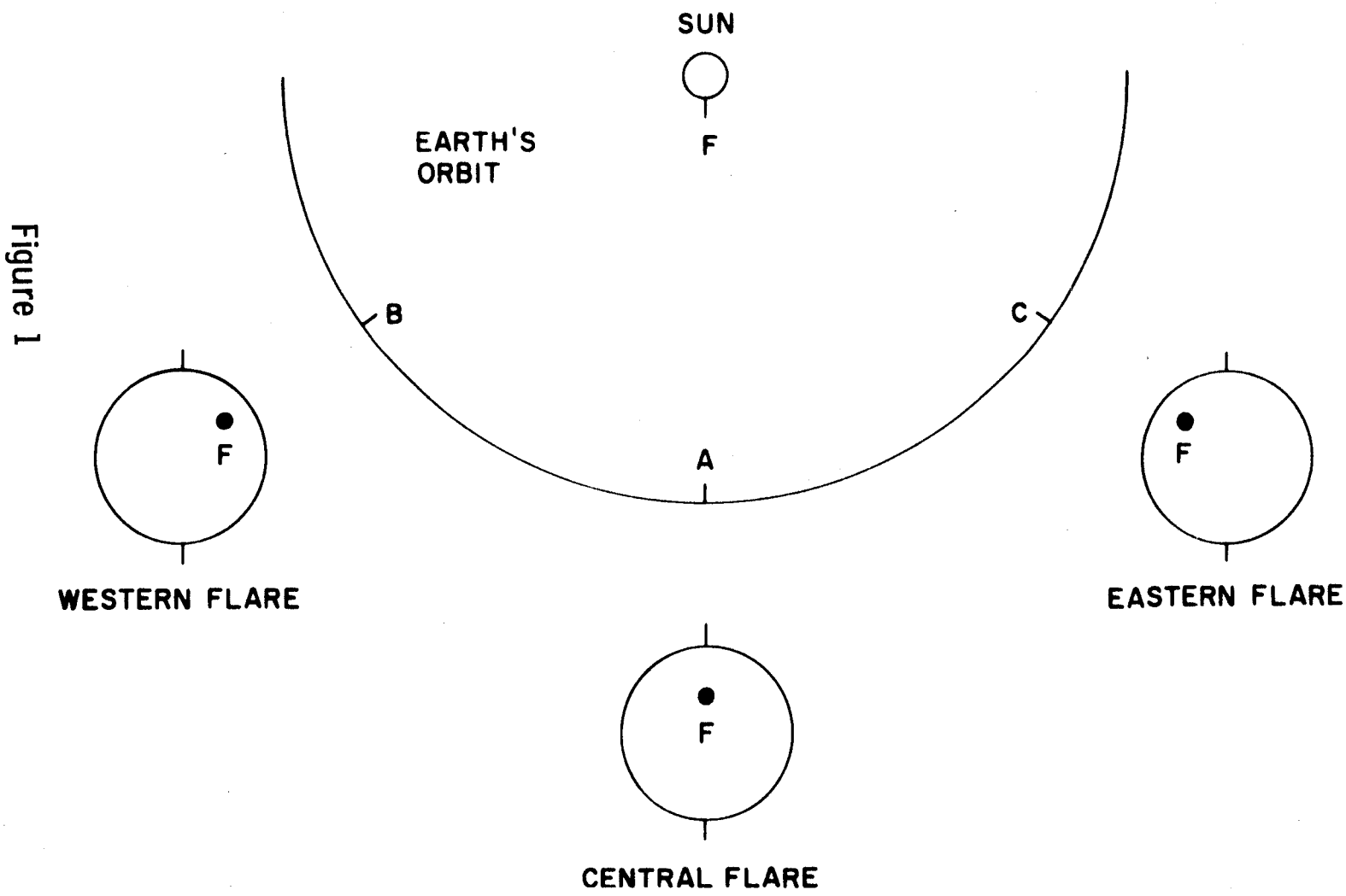
SUN
F
EARTH'S
ORBIT
B
C
A
F
WESTERN FLARE
F
EASTERN FLARE
F
CENTRAL FLARE

Figure 1

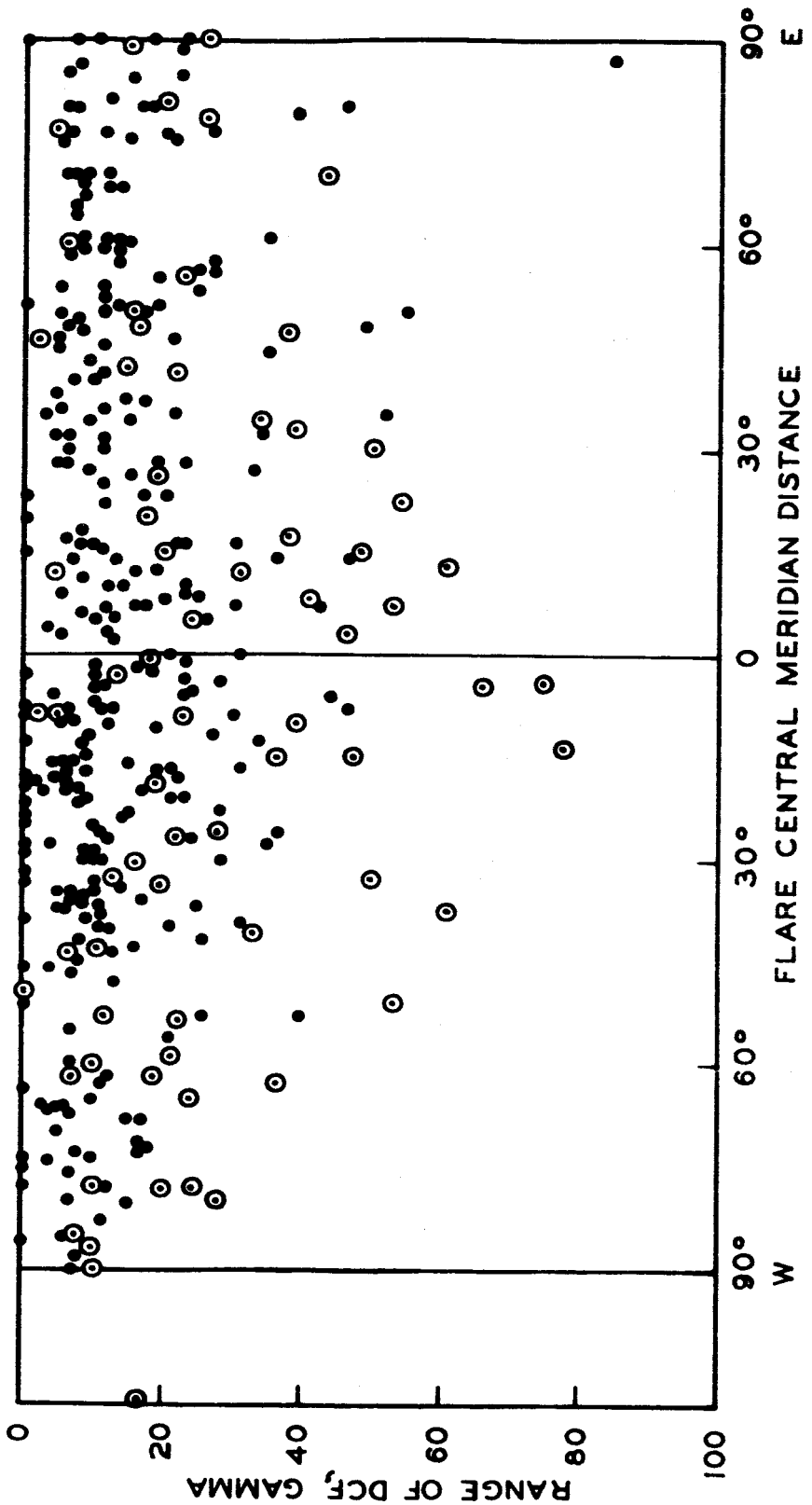
RANGE OF DCF, GAMMA
0
20
40
60
80
100
90° W
60°
30°
0
30°
60°
90° E
FLARE CENTRAL MERIDIAN DISTANCE

Figure 2

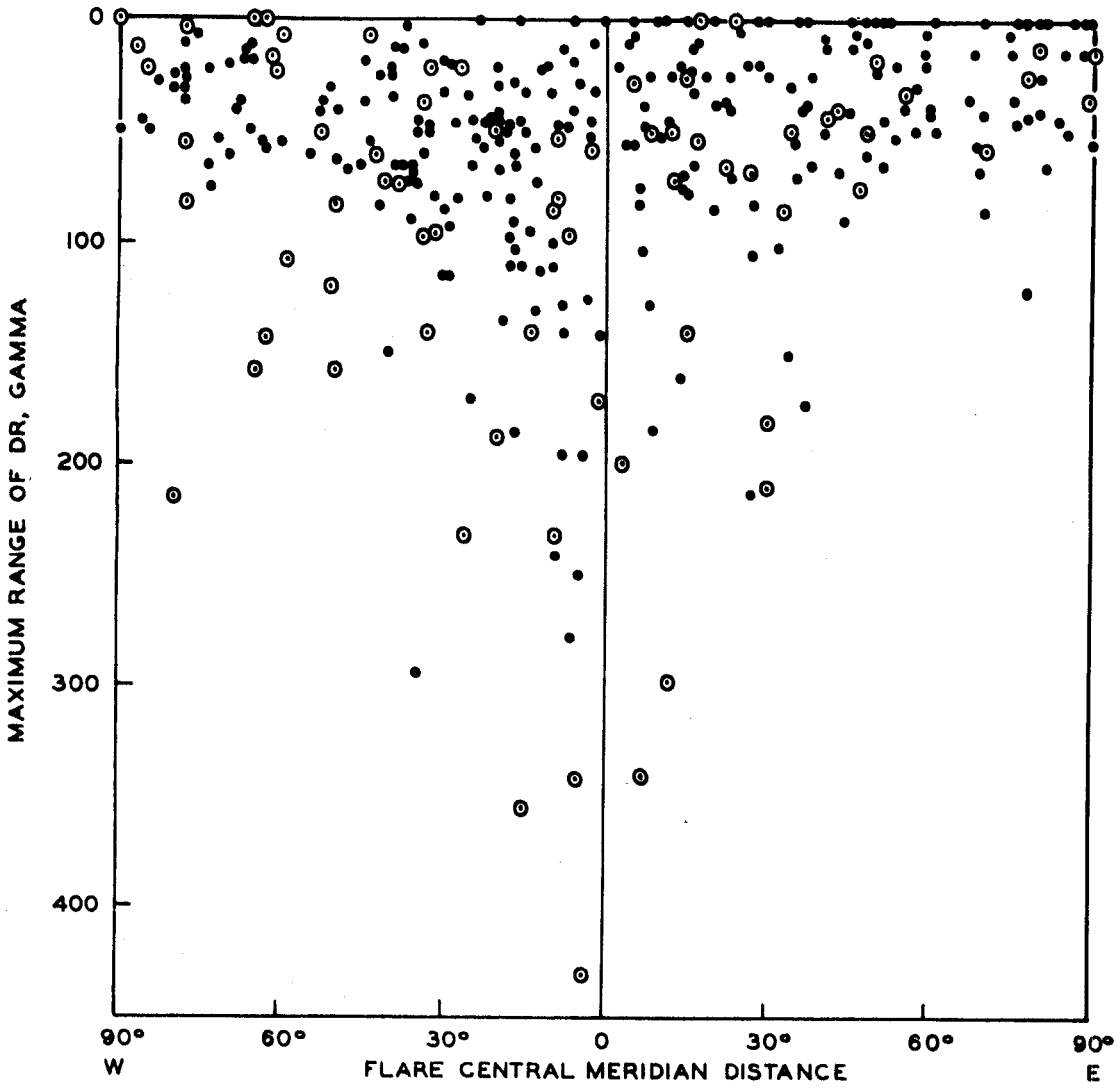
0
100
200
300
400
MAXIMUM RANGE OF DR, GAMMA
90°
W
60°
30°
0
30°
60°
90°
E
FLARE CENTRAL MERIDIAN DISTANCE

Figure 3

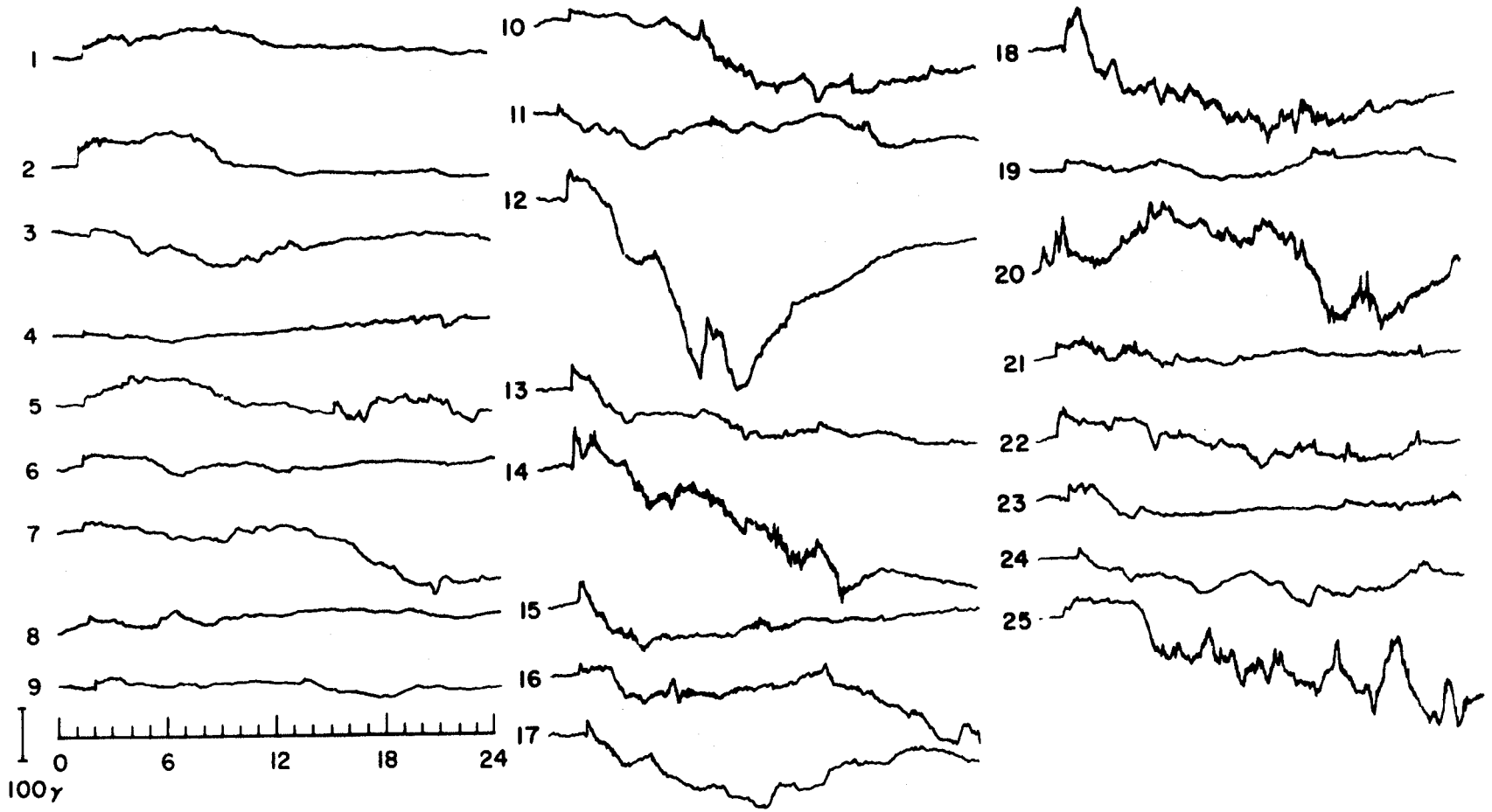
1
2
3
4
5
6
7
8
9
10
11
12
13
14
15
16
17
18
19
20
21
22
23
24
25
0
6
12
18
24
100γ

Figure 4

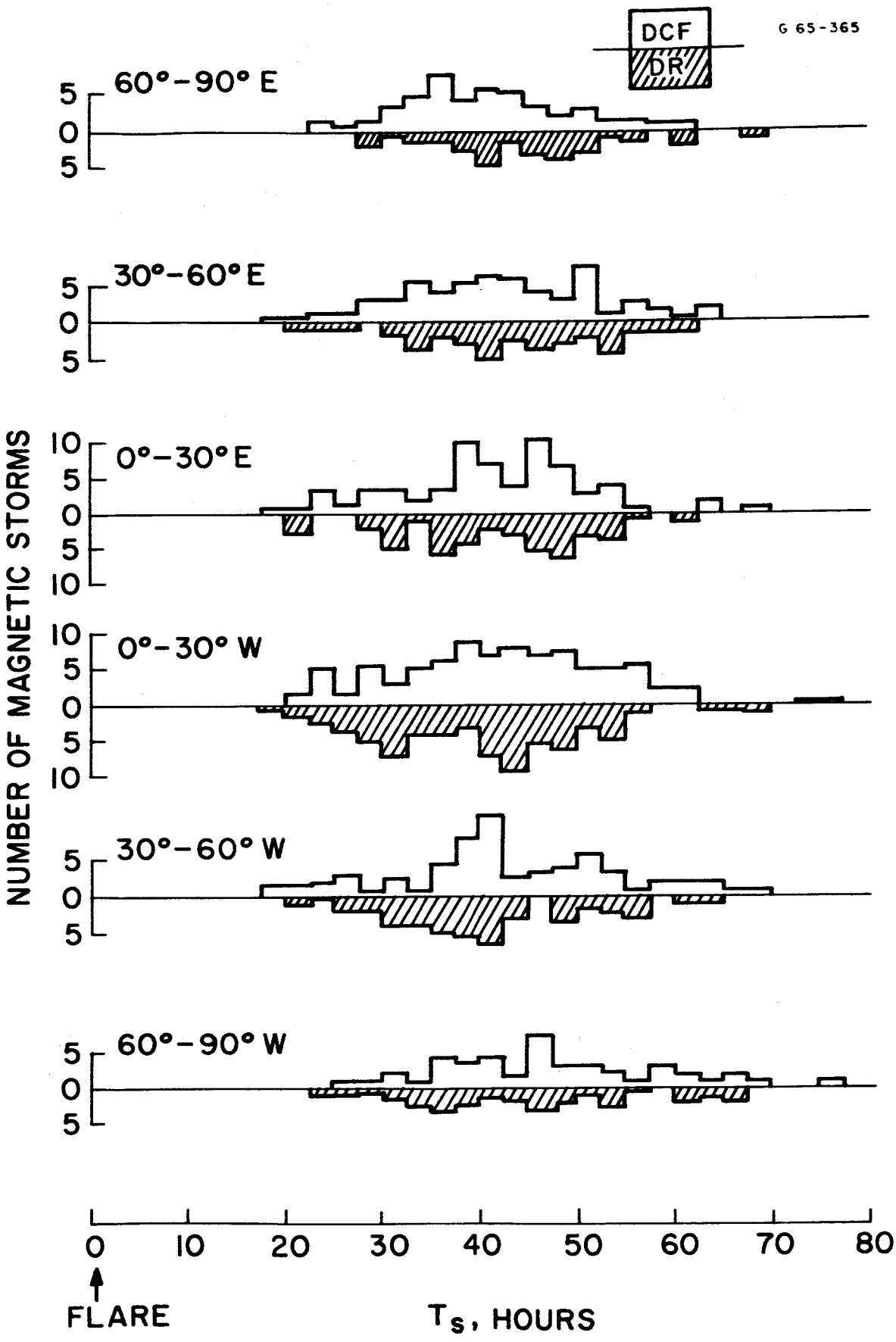
DCF
DR
G 65-365
60°-90° E
30°-60° E
0°-30° E
0°-30° W
30°-60° W
60°-90° W
NUMBER OF MAGNETIC STORMS
5
0
5
10
0
10
20
30
40
50
60
70
80
FLARE
T_S, HOURS

Figure 5

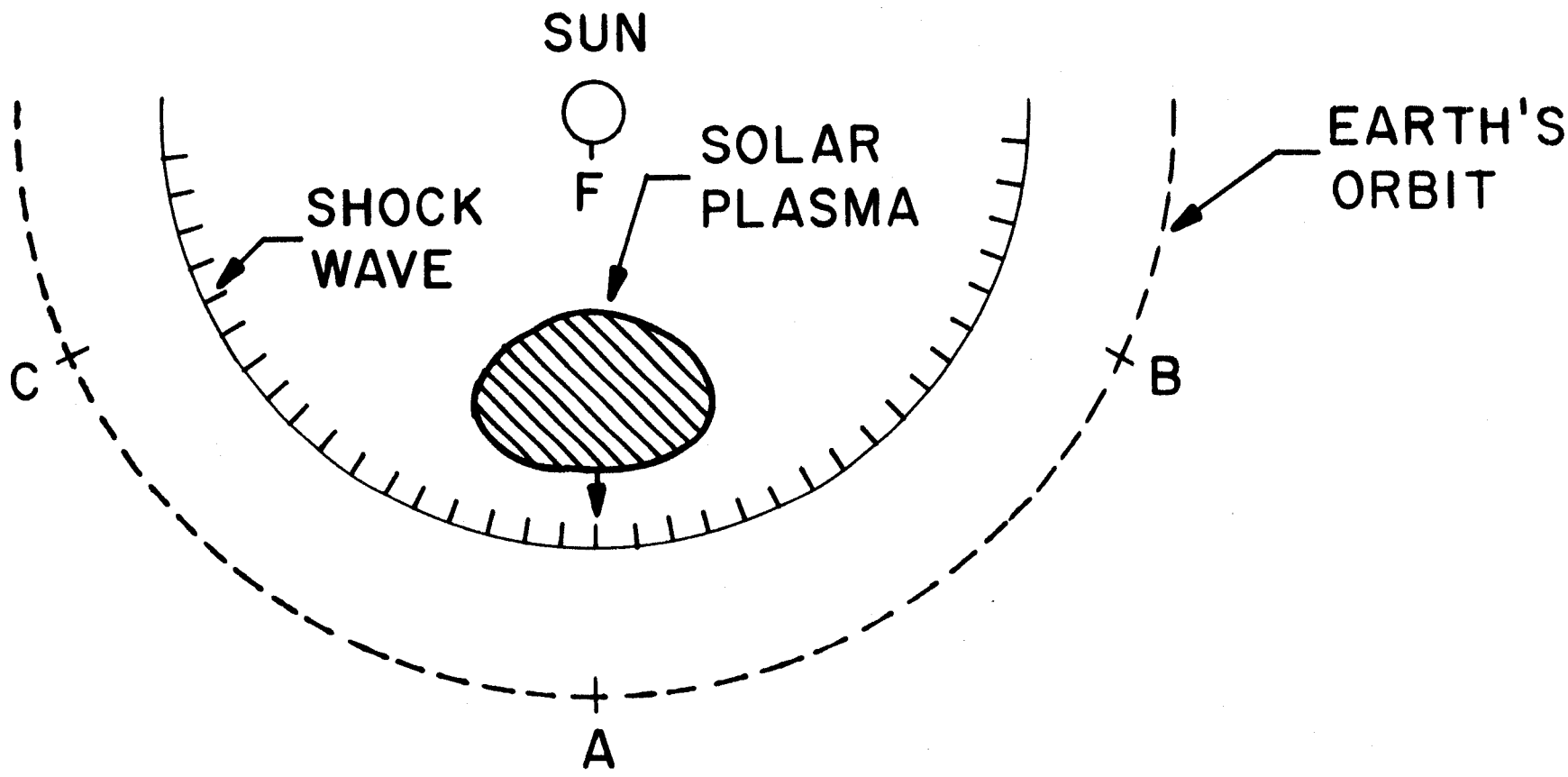

Figure 6

G 66-253

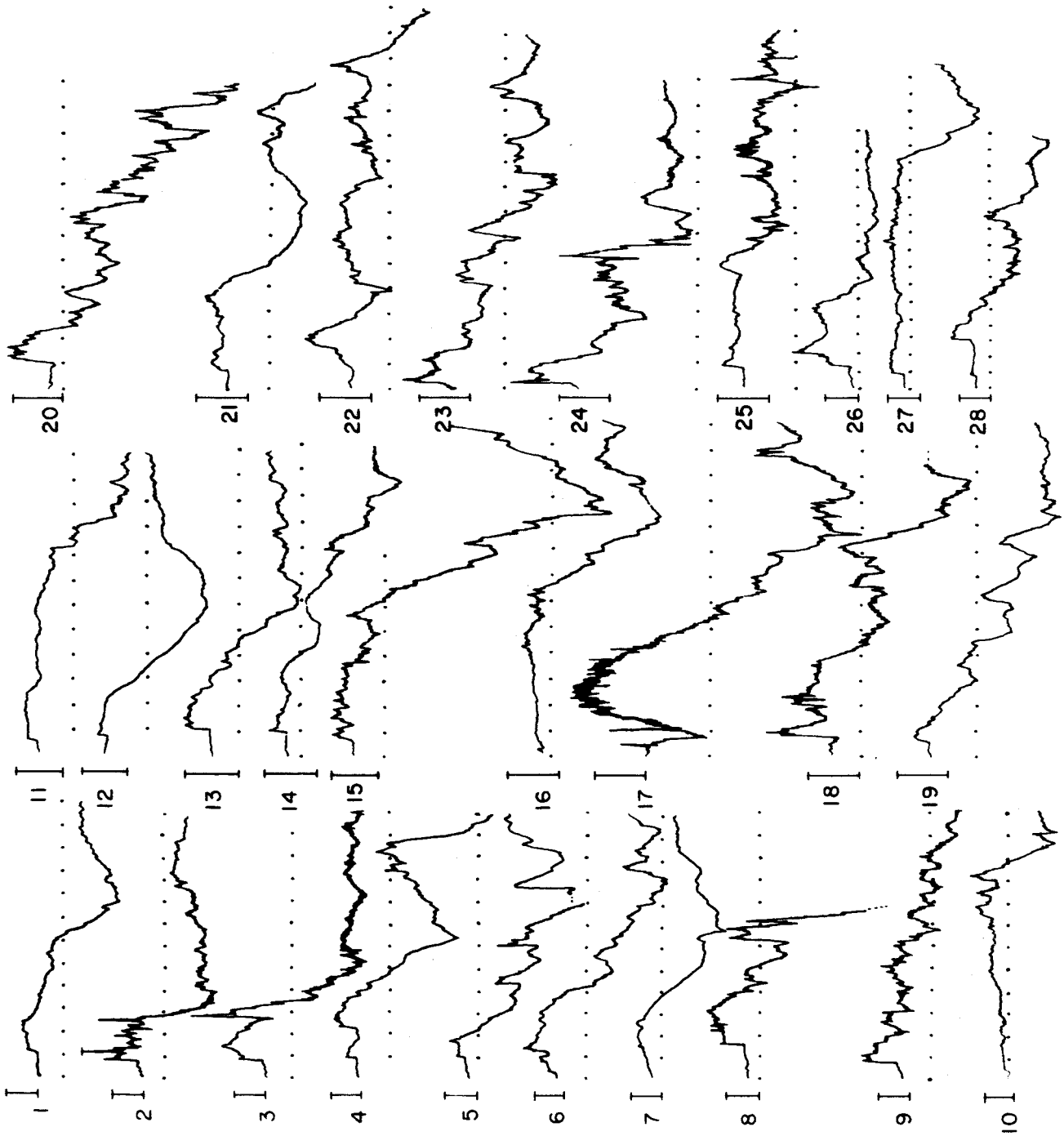

Figure 7

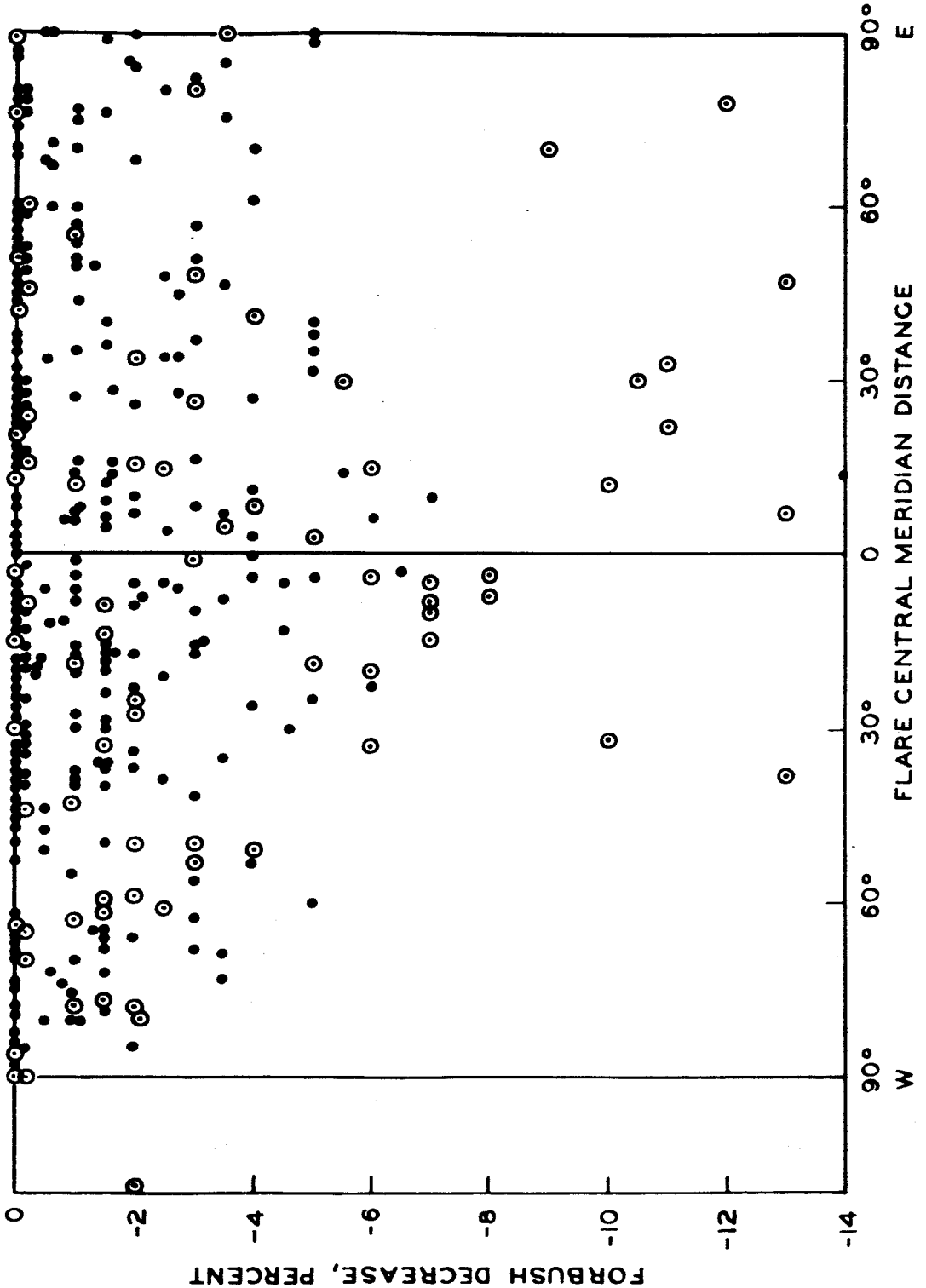
FORBUSH DECREASE, PERCENT
0
-2
-4
-6
-8
-10
-12
-14
90° W
60°
30°
0
30°
60°
90° E
FLARE CENTRAL MERIDIAN DISTANCE

Figure 8

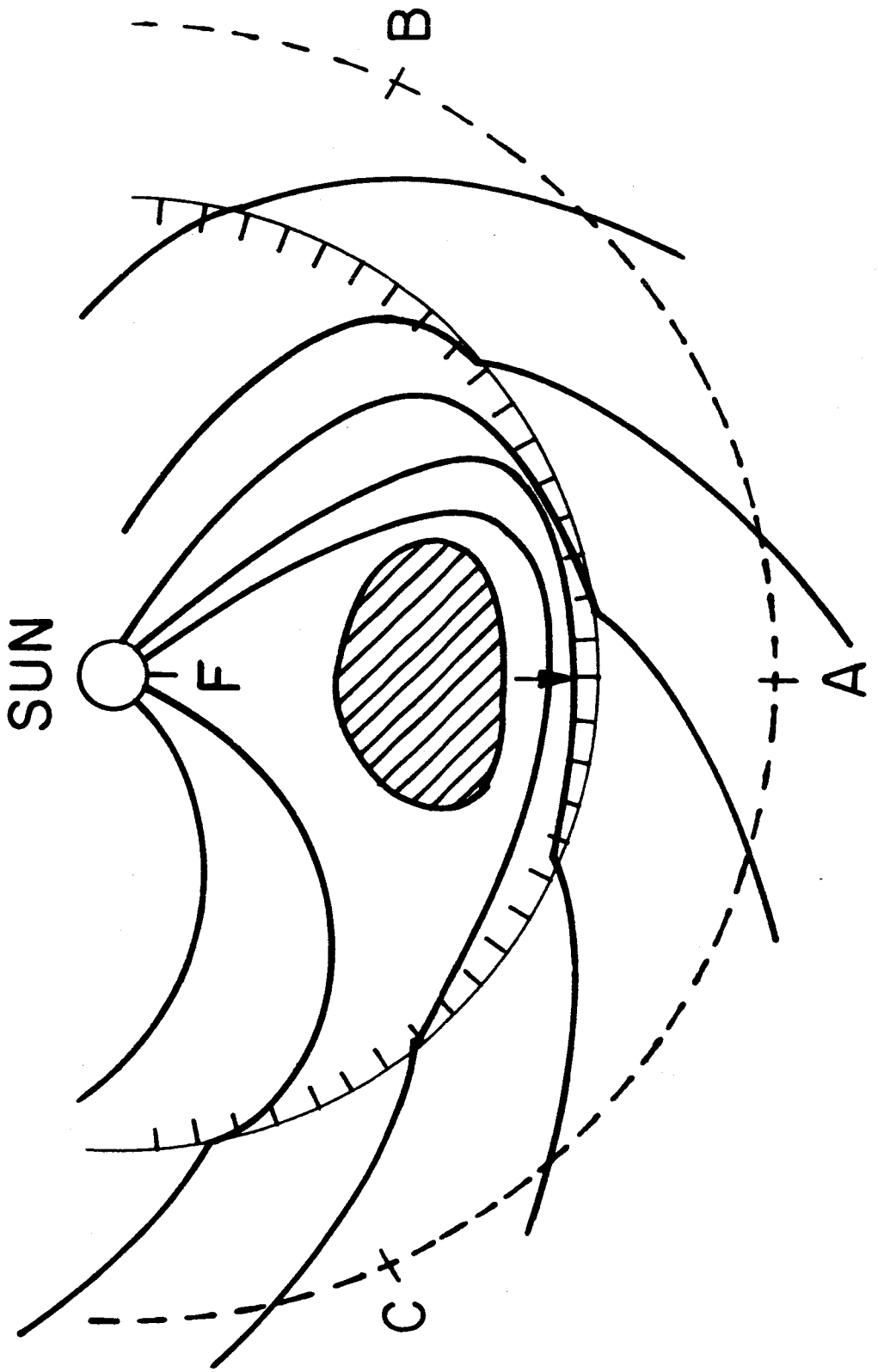

Figure 9

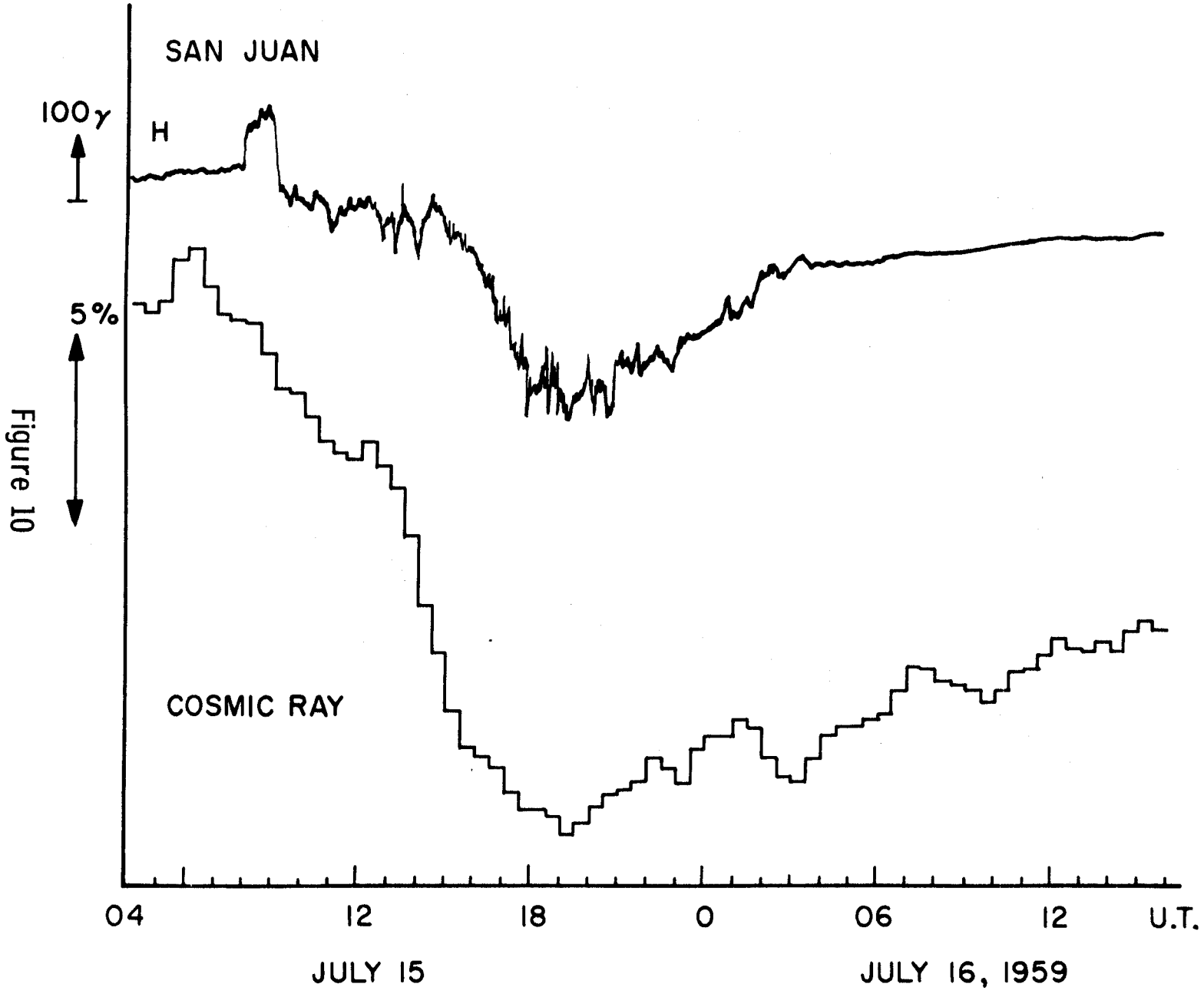
SAN JUAN
100γ
H
5%
COSMIC RAY
04
12
18
0
06
12
U.T.
JULY 15
JULY 16, 1959

Figure 10

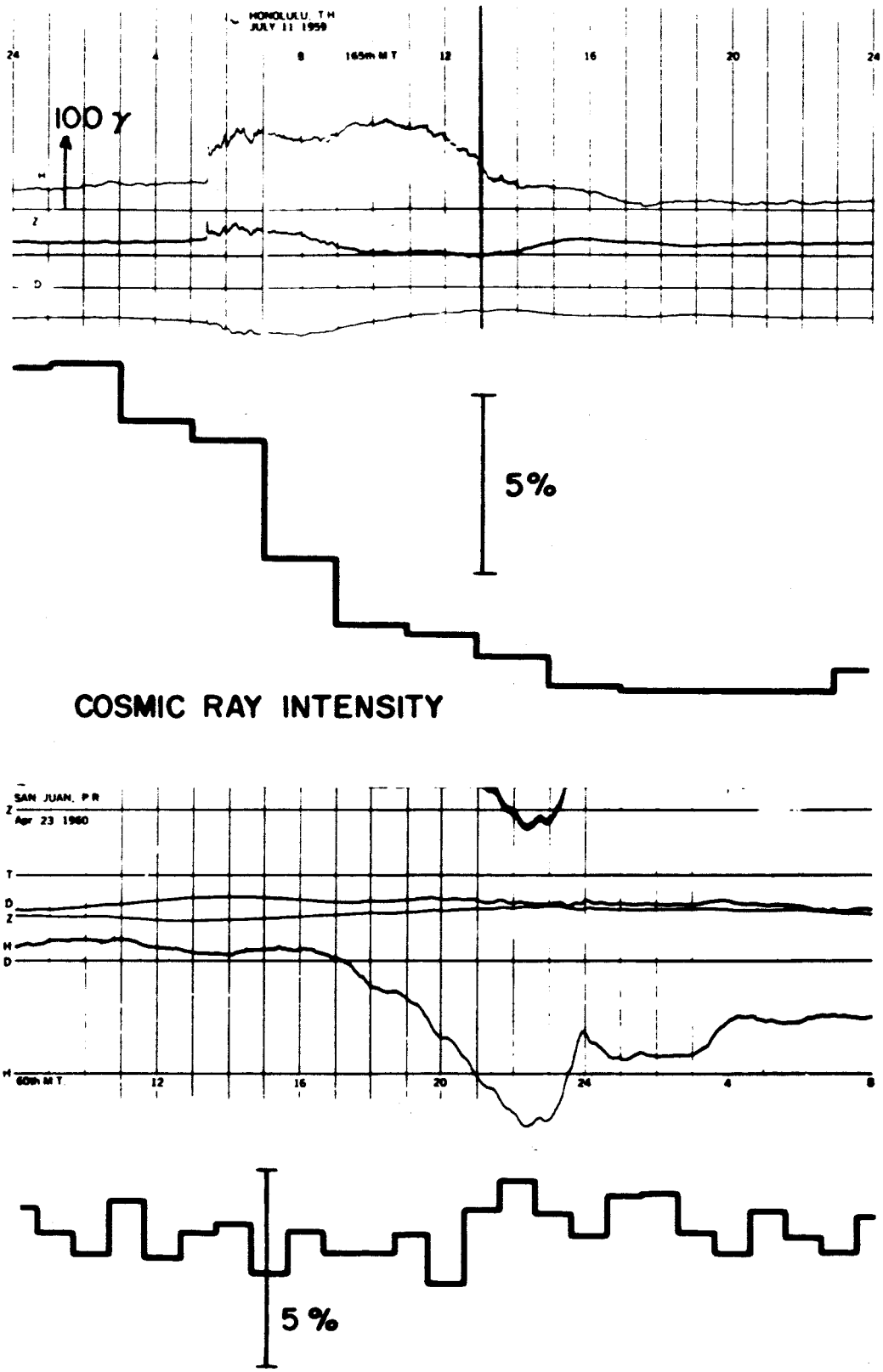
HONOLULU, T H
JULY 11 1959
24
4
8
16
20
24
100 γ
H
Z
D
5%
COSMIC RAY INTENSITY
SAN JUAN, P R
Apr 23 1960
Z
T
D
Z
H
D
H
60th M T
12
16
20
24
4
8
5 %

Figure 11

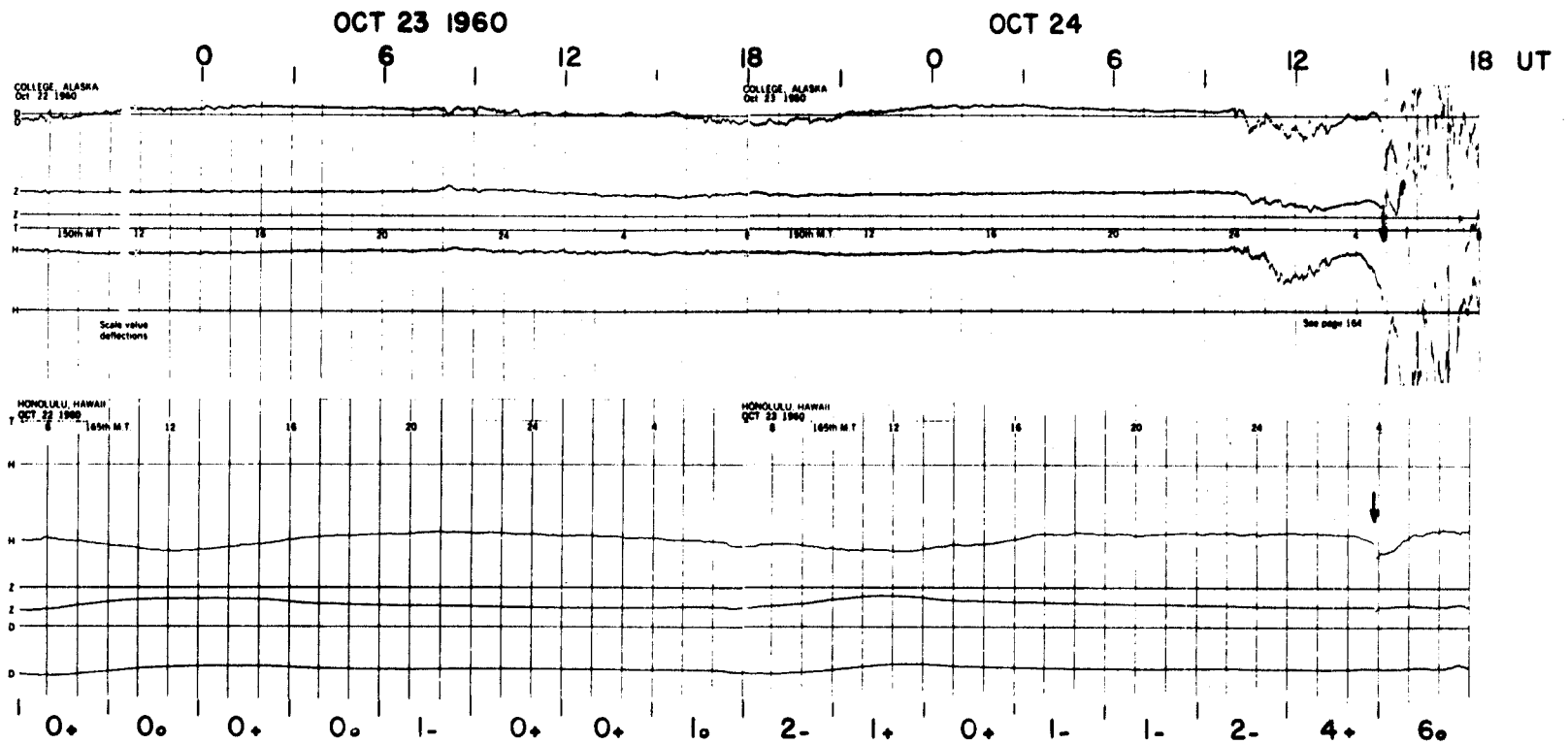
OCT 23 1960
OCT 24
0
6
12
18
0
6
12
18 UT
COLLEGE, ALASKA
Oct 22 1960
COLLEGE, ALASKA
Oct 23 1960
D
Z
Z
T
150th M.T
H
H
Scale value deflections
See page 164
HONOLULU, HAWAII
OCT 22 1960
HONOLULU, HAWAII
OCT 23 1960
165th M.T
H
H
Z
Z
D
D
0+ 0o 0+ 0o 1- 0+ 0+ 1o 2- 1+ 0+ 1- 1- 2- 4+ 6o

Figure 12

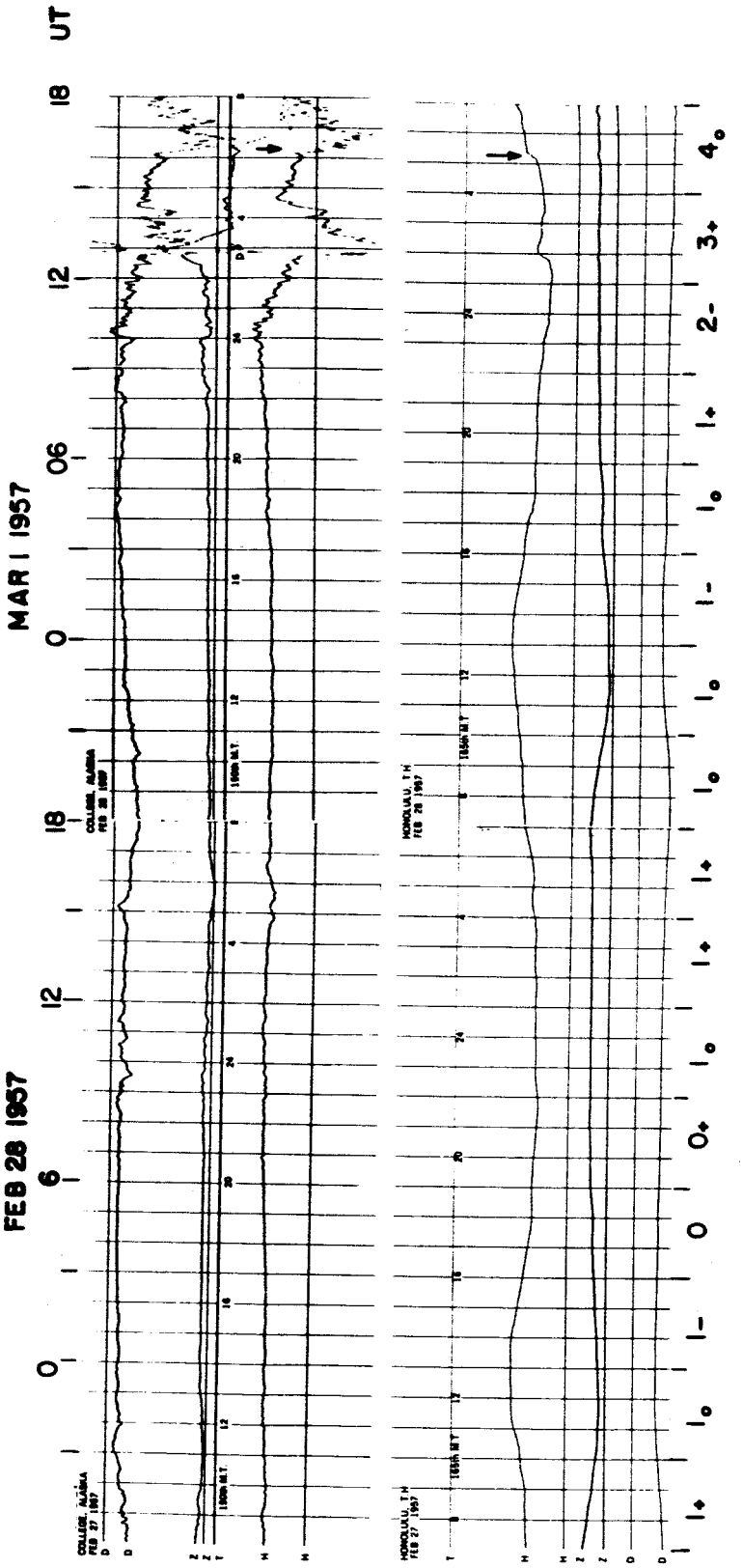

Figure 13